Topological Analysis on the Degree of Complexation and Viscosity of Polymer Complexes

Jung Mo Son and Hyungsuk Pak

Department of Chemistry, Seoul National University, Seoul 151-742, Korea
Received July 6, 1995

A topological theory has been introduced to evaluate the degree of complexation and the viscosity of polymer complexes by extending the theory of Iliopoulos and Audebert for aqueous polymer solutions. The previous theory of Iliopoulos and Audebert has offered only a semiquantitative theoretical model for polymer complex systems, whereas our present work gives a general theoretical model applicable to all the polymer complex systems. Their theories considered only the physical property term caused by the displacement of complexed points between polymer solute chains, while our theory deals with all the physical effects, caused by the displacement of complexed points entangled points in polymer solute chains. There have been predicted the characteristics of physical properties from the expression. It is exposed that the predictive values show good agreement with the experimental data for polymer complexes.

Introduction

Recently topological theories make a great contribution to the study of various physical properties including the elasticity of polymers. It is well known that the theories which have systematically studied the rubber elasticity so far are the phantom network theories[1~6] headed by Flory *et al.* and the topological network theories[7~12] headed by Iwata *et al.* Phantom network theories have recently retrograded since these theories have dealt with the energies of rubber elasticity as only functions of the end-to-end distance between junction points, and have not considered the entanglement effect between chains. On the other hand, since topological network theories have explained the effect very well, these theories have remarkably developed. Iwata has explained the various phenomena of rubber elasticity by applying topological theories to the polymer systems consisting of only a single kind of polymers.[10~12] The models which he has studied are mainly confined to the SCL (simple cubic lattice) ones,[11~12] but for the THL (tetrahedral lattice) ones he did notobtain transformation matrices and related topological contribution terms of entropy. By applying his initial topological network theories to the THL model, we analyze the theory of Iliopoulos and Audebert of polymer complexes in view of topological approach. The question of how the viscosity caused by strands is related to the interaction between chains of polymer systems has systematically examined. Here, a topological theory for polymer complexes has been evolved by assuming that the polymer complexes have the structure of the THL model. It is supposed that all the junction points of polymer complexes form the THL model for some average time interval.

In the present work, the physical property term caused by interaction between strands has been topologically derived based upon the THL model. We have topologically extended the theory of Iliopoulos and Audebert[13] by combining the topological terms with the ones caused by displacement of junction points. In the result, a discrepancy between the original theory of Iliopoulos and Audebert and experimental data is removed. The predictive values are in good agreements with the experimental data.

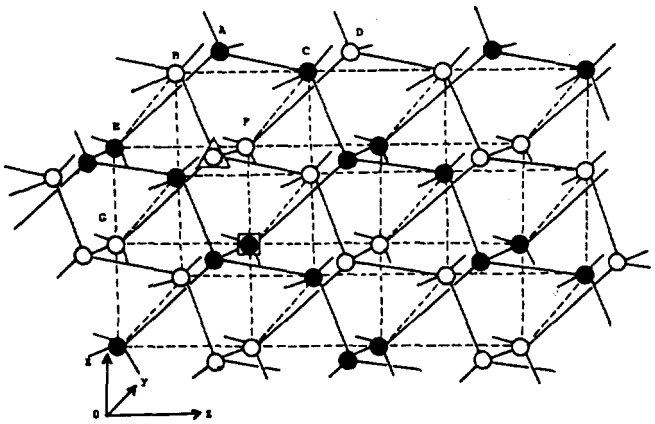

Figure 1. The three dimentional structure of the THL (tetrahedral lattice) model, where solid lines denote strands and small circles represent junction points. The black closed circles including *A* and *C* represent the sets of junction points of polyacid solute molecules, and white open circles *B* and *D* represent those of polybase solute molecules. A junction point, J_{∞}, is plotted as the junction point surrounded with a regular square, while a junction point, J_{∞}, is plotted as that with a regular triangle. The length of $\overline{BE}$, $\overline{EF}$, and $\overline{EG}$ is all two without unit.

THL Model

The THL(tetrahedral lattice) model is the one in which the junction points of polymer networks are located at the points of a body-centered cubic lattice, and in which the arrangement of four strands projected from each junction point always takes the tetrahedral structure. The picture of the three dimensional structure of the THL model is given in Figure 1, where solid lines denote linearly compressed strands and small circles represent junction points.

This THL model has been known as the body-centered-cubic lattice(BCL) one by our previous work,[14] The distribution functions and transformation matrices of the THL model had already been offered by our previous work.[14~16] The study about the physical properties of polymer blends and

polymer solutions had also been carried out, based on the THL model in our previous works.[17~18]

In the present work, the contribution terms due to the degree of complexation and the viscosity caused by interaction between polymer strands are derived from topological distribution functions by asssuming that the structure of polymer complexes forms a large aggregate of the THL model.

All the systems we consider in this work are aqueous polymer solutions in which two kinds of polymers (*i.e.*, polyacids and polybases)exist as solutes and water, as a solvent. Especially one of two kind of polymer solutes is a polyacid such as poly(acrylic acid)(PAA), and the other is a polybase such as poly(ethylene oxide)(PEO), poly(vinylmethyl ether) (PVME), and poly(N-vinyl-2-pyrrolidone).[13]

In the THL model, it is supposed that a polyacid solute chain aggregate is regularly arranged at the lattice points, in turn with the polybase chain aggregate. For example, in Figure 1, the black closed circles including A and C represent the sets of junction points of polyacid solute molecules, and the white open circles including B and D represent those of polybase solvent molecules. Especially, in the case that solute molecules have lower molecular weight which does not form cross-link, the open circles represent the sites to which the end point of solute molecules attach. Shortly speaking, the network structure of the THL model is composed of the aggregate of polyacid and polybase solute molecules, and water fills evenly all the vacant space of the network structure of the THL model. In each chain aggregate, junction points are classified into two categories according to the methods of their combination with neighboring strands. One is the set of junction points corresponding to the apexes of lattices (*i.e.*, the junction point surrounded with a regular square of Figure 1), and the other to the body centers of lattices (*i.e.*, the junction point surrounded with a regular triangle of Figure 1).

Let J_{ev}'s be junction points of the former and J_{od}'s the latter. For either J_{ev}'s or J_{od}'s, two different spatial orientations per junction point can be allocated in the way of combination with four neighboring strands around a given junction point. The effects of these two arrangements, however, are essentially identical in view of contribution to the free energy of the system, so it dosen't matter which of them is chosen in going on discussing. Usually it is convenient to select a J_{ev} in the central part of the system as an origin of the coordinates.

Conveniently, if the length of an edge of lattices is taken as two (*i.e.*, the distances of $\overline{BE}$, $\overline{EF}$, and $\overline{EG}$ in Figure 1 are all two), the coordinates of every junction point can be readily described as the set of three components having only values of integers. Figure 2 represents the characteristic combination modes of strands around the general junction points J_{ev}'s and J_{od}'s, and shows the spatial orientations of strands defined on the basis of a J_{ev}, in addition to the coordinates of junction points.

Independently of J_{ev} or J_{od}, if l is taken as a position vector, the equations give its components and their areas as follows;

$$\begin{aligned} &l=(i,\ j,\ k)\\ &i=-I,\ -I+1,\ \cdots,\ I-1,\ I\\ &j=-J,\ -J+1,\ \cdots,\ J-1,\ J\\ &k=-K,\ -K+1,\ \cdots,\ K-1,\ K \end{aligned} \tag{1}$$

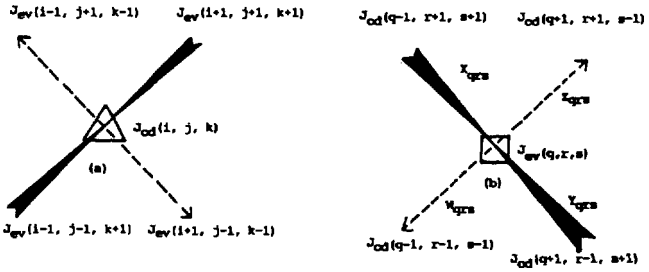

Figure 2. The characteristic combination modes of strands around the general junction points J_{od} (a) and J_{ev} (b). In this picture there are shown the spatial orientations of strands defined on the basis of a J_{ev}, in addition to the coordinates of junction points.

where I, J, and K all take the values of positive integers.

Note that the components of every J_{ev} all have values of even integers, and that those of every J_{od} have only values of odd integers. The spatial orientations of all the strands in the system are deduced to only four, as plotted in Figure 2(b). Conveniently, let σ_l or $\sigma_{i,j,k}$ ($\sigma=X,\ Y,\ Z,$ and W) be a symbol which represents a strand. Then the four spatial-orientations of strands in the system are defined as

$$\begin{aligned} &X_{i,j,k}=\text{strand from } J_{ev}(i,j,k) \text{ to } J_{od}(i-1,\ j+1,\ k+1)\\ &Y_{i,j,k}=\text{strand from } J_{ev}(i,j,k) \text{ to } J_{od}(i+1,\ j-1,\ k+1)\\ &Z_{i,j,k}=\text{strand from } J_{ev}(i,j,k) \text{ to } J_{od}(i+1,\ j+1,\ k-1)\\ &W_{i,j,k}=\text{strand from } J_{ev}(i,j,k) \text{ to } J_{od}(i-1,\ j-1,\ k-1) \end{aligned} \tag{2}$$

The picture for these orientations is given in Figure 2(b).

For the THL model, the single contact probability between two strands, $g_p(r_i)$, and the double one between two strands, $h_p(r_i)$, are given by[14~18]

$$\begin{aligned} g_p(r_i)&=m^{-2}\sum_{\mu=1}^{m^2} P_{ph}(O_\mu|r_i)\\ h_p(r_i)&=m^{-2}[g_p(r_i)]^{-1}\sum_{\mu=1}^{m^2}\sum_{\mu'=1}^{m^2} P_{ph}(O_{\mu\mu'}|r_i) \end{aligned} \tag{3}$$

where m is the number of submolecules in a strand, and r_i is the position vector of the ith strand from the reference junction point. $P_{ph}(O_\mu|r_i)$ is the single contact distribution function between chains, and $P_{ph}(O_{\mu\mu'}|r_i)$ is the double one of the phantom network. The detailed terms of$P_{ph}(O_\mu|r_i)$ and $P_{ph}(O_{\mu\mu'}|r_i)$ have been offered in Refs. 14-18.

The number of distinguishable arrangement caused by single contact between all the strands, Ω_g, is given by

$$\begin{aligned} \Omega_g&=(1/n_1!)\prod_{i=1}^{n_1-1} g_p(r_i)\\ &=(1/n_1!)\prod_{i=1}^{n_1-1}\left(g_p(r_i)^{m-2}\sum_{\mu=1}^{m^2} P_{ph}(O_\mu|r_i)\right) \end{aligned} \tag{4}$$

where n_i is the number of lattice sites available to the $(i+1)$ th strand. The number of distinguishable arrangement caused by double contact between all the strands, Ω_h, is represented by

$$\Omega_h=(1/n_1!)\prod_{i=1}^{n_1-1} h_p(r_i)$$

$$=(1/n_1!)\prod_{i=1}^{n_1-1}\left(\left(g_p(r_i)^{m-2}\right)^{-1}\sum_{\mu=1}^{m^2}\sum_{\mu'=1}^{m^2}P_{\mu\mu}(O_{\mu\mu'}|r_i)\right) \quad (5)$$

Evolving Eqs. (4) and (5) by following the procedure offered in Refs. 14-18, the equations for Ω_g and Ω_h are obtained as follows;

$$\Omega_g=\Omega_{FH}\in m\ \ln((1-\phi)^{1/4}/(1-\phi-0.5\phi^2)^{3/4}) \quad (6)$$

and

$$\Omega_h=\Omega_{FH}\in m\ \ln((1-\phi)^{1/4}/(1-\phi-0.5\phi^2)^{1/2}) \quad (7)$$

where $\phi(r)$ is the local polymer volume fraction remote from the reference point by r. The number of distinguishable of the Flory-Huggins's theory,[19], Ω^{FH}, and the variable $\in$ are given by

$$\Omega_{FH}=(1/n_1!)\ (\{z(z-1)^{m-2}\}/n_o^{m-1})^{n_1} \quad (8)$$

and

$$\in=(1/4)\ (\nabla^2\phi)_o\ a^2n_o \quad (9)$$

where z is the coordination number of the lattice, n_o is the number of the lattice sites, and a is the length of a strand. The number 4 in the denomenator of Eq. (9) represents four directions of the strands attached to junction points. Thus the total number of topologically distinguishable arrangement caused by interaction between all the strands, Ω_{top}, is given by

$$\Omega_{top}=\Omega_g+\Omega_h$$
$$=\Omega_{FH}\in m\ \ln((1-\phi)^{1/2}/(1-\phi-0.5\phi^2)^{5/4}) \quad (10)$$

Eq. (10) is a very valuable expression obtained by expanding the topological theory of Iwata to the THL model.

For phantom network theories, the entropy of polymer systems has been analyzed so far only by the contribution terms caused by displacement of junction points. In topological network theories, the change of entropy and free energy has been more completely considered by adding the contribution terms of entropy caused by interaction between strands to those caused by displacement of junction points.

Eq. (10) has important meanings because of the fact that it offers the source of topological entropy based upon the structure of the polymer network of the THL model. In the next section, we consider how Eq. (10) improves the theory of Iliopoulos and Audebert, how it removes the discrepancy between predictive values and experimental data, and how it explains good agreement between theoretical values and experimental data.

The complexation between two kinds of solutes (*i.e.*, polyacid and polybase) arises from the result of hydrogen bonds between the related polyacids and polybases. The degree of complexation and the viscosity between strands are affected by the interaction caused by entanglement between strands in the polymer networks. For the theory of Iliopoulos and Audebert, there was not considered the topological effect caused by interaction between strands. In the case of their theory for polyacid and polybase solutes, there has been dealt only the special case that all the solutes do not form polymer networks, and there has not been considered the contribution to the degree of complexation and the viscosity of phantom networks according to the displacement of junction points of polymer networks.

Essentially the greater the length of a chain is, the greater the tendency to form polymer networks is, and usually it is apt to have the network structure composed of junction points of the four functional type. The theory of Iliopoulos and Audebert is not only a semiquantitive theory on polymer complexes but also an incomplete theory having not considered the contributional effect between junction points and strands. In the present work, we modify an incomplete part of theirs, based upon topological network theories, and offer a general and inclusive theory applicable to all the polymer complexes.

Topological Analysis of the Iliopoulos and Audebert's Theory

Consider a polymer network of the THL model, composed of n_A polyacid molecules and n_B polybase molecules in the solution of the volume V. Letting the number of junction points of polyacid chains be n_{AJ}, and that of polybase chains be n_{BJ}, then the total number of junction points of the polymer network, n_J, is given by

$$n_J=n_{AJ}+n_{BJ} \quad (11)$$

The partition function of junction points in a phantom network, Ω_{ph}, is given by[18~19]

$$\Omega_{ph}=\Omega_{FH}(1+(\in m/2)\ \ln[1-\bar{\phi}]^{-1}) \quad (12)$$

where $\bar{\phi}$ is the averaged polymer concentration, m is the number of the submolecules contained in a strand, and Ω_{ph} is given in Eq. (8). The total partition function of the mixed systems, Ω, is obtained by adding Eq. (10) to Eq. (12). Namely,

$$\Omega=\Omega_{ph}+\Omega_{top}$$
$$=\Omega_{FH}(1+(5\in m/4)\ \ln\ [1-\bar{\phi}-\bar{\phi}^2]^{-1}) \quad (13)$$

For two polymer solutes, let a given A-type polymer be represented as polyA, and a long B-type macromolecule be represented as polyB. It is noted that our study is confined in the systems of reversible polymer complexes stabilized through weak interactions. For such a situation, the cooperative effect increases. This shows that oligomers of a given polyA cannot be complexed with polyB if the size of polyA chain is not large enough (*i.e.*, the degree of polymerization is smaller than a critical chain length, l_c). More concretely we treat the situation of a mixture of a homopolymer (polyB) with a random copolymer (copolyAX) where X is a unit which cannot interact with B units. Such a situation is showed by Scheme 1.

It is known that the association between complementary polyacid and polybase chains is governed by the cooperative formation of hydrogen bonds as it was claimed by Kabanov and others.[20~28]

The polymer complexes we study are confined in polyacid polybase systems, for instance, aqueous solution mixture of poly(acrylic acid) (PAA) with polybases: poly(ethylene oxide) (PEO), poly(vinyl-methylether) (PVME) or poly(*N*-vinyl-2-pyrrolidone) (PVP).

For such systems, PAA behaves as a copolymer since it contains complexable acid groups, COOH, forming hydrogen

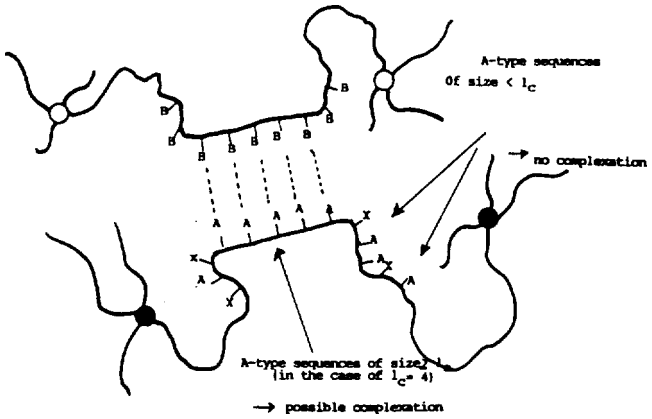

Scheme 1. The condition on which the complexation can arise or not among strands. The open circles represent the junction points belonging to the polybase chain network, while the closed circles represent those belonging to the polyacid chain network. The complexation between strand sarises when the length of a polyacid sequence is equal or longer than the critical chain length, l_c.

bonds with the oxygen atoms of the polybases and uncomplexable acrylate groups, COO^-.

Degree of Complexation

For water solution, it is known that the complexation of a polybase with a weak polyacid (for instance PAA) induces a shift on the dissociation equilibrium of the acid groups. Conveniently, the effective degree of complexation, θ, is defined as follows;

$$\theta=\frac{\text{concentration in PAA units involved in the complex}}{\text{total concentration in PAA units}} \tag{14}$$

Generally speaking, the complex formation can be described as an equilibrium between free and complexed units of the macromolecules. Actually, the conception of the complexation involving only individual units is not suitable because the affinity of an *A*-type unit for the *B*-type units depends on the length of the sequence which includes the *A*-type unit considered.

It is regarded that a description of the system as an equilibrium between complexed and uncomplexed sequences is more realistic. Since very short *A*-type sequences have no affinity for polyB chains, even for the naive description according to Scheme 1, the problem is not so simple. This affinity becomes noticeable when the sequence size is equal to the critical chain length, l_c, and it increases with the sequence size.

Consider a simplified model by considering that each PAA chain contains only two types of sequences: short uncomplexable sequences and sequences with a size larger than l_c, complexable and isoreactive.

Let the average degree of polymerization of polymers in the system be N, and the ratio of inactive groups in the copolyAX chain be $p=[X]/([A]+[X])$. From given values of the physicochemical parameters N, l_c, and p, we can calculate the number B of acid sequences of size equal or higher than l_c involved in a PAA chain and the total number of acid groups they contain. Thus, the average length, L, of acid sequences having a size longer than l_c can be determined;

$$L=\frac{\text{total number of COOH in acid sequences of length larger than } l_c}{B} \tag{15}$$

In Scheme 2, the simplified picture of the PAA chain is illustrated. It is assumed that each macromolecule contains B complexable sequences of size L regularly alternated with uncomplexable sequences (size M) containing acrylate groups and acid sequences of length shorter than l_c.

It may be assumed that the proposed structure of the copolymer does not take a static distribution of acid sequences on the PAA chain. In such a situation, a given acid group, complexed at time t, can be free or in the acrylate form at $t+dt$. The average number of complexed sequences, however, remains invariant with time for a fixed composition of the system.

It is supposed that the eletrostatic repulsion between vicinal acylate groups may be opposed to the random distribution of acid sequences on the PAA chain, but for the low content of COO^- groups used, the random distribution must not be affected.

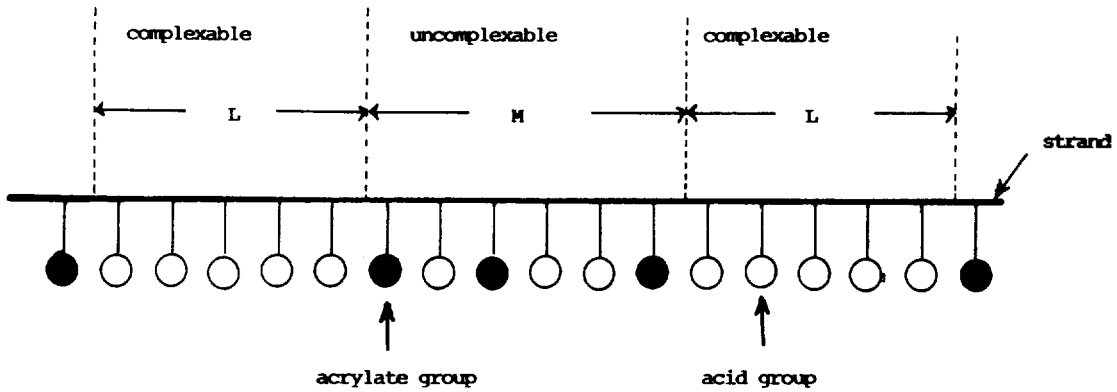

Scheme 2. The structure of a strand in the polymer network. It is assumed that a strand is averagely composed of n complexable sequences of length L and m uncomplexable sequences of length M.

In such a situation, complexation can be examined as an equilibrium between acid and base complexable sequences as follows;

$$\left(\frac{\text{free complexable}}{\text{sequences of PAA}}\right)+\left(\frac{\text{free complexable}}{\text{sequences of polybase}}\right) \underset{}{\overset{K_s}{\rightleftharpoons}} \left(\frac{\text{complexed}}{\text{sequences}}\right) \tag{16}$$

The degree of comlexation, θ, is then related to the complexation constant, K_s, by

$$K_s=\frac{C_{SC}}{(C_{SA}-C_{SC})(C_{SB}-C_{SC})} \tag{17}$$

where C_{SA} is the initial total concentration of complexable sequences of PAA, C_{SB} is that of complexable sequences of polybase, and C_{SC} is the concentration of complexed sequences at equilibrium. The concentrations C_{SA}, C_{SB}, and C_{SC} are the functions of known experimental parameters such as the degree of complexation, θ, the concentration of polyacid, C_A (represented as [COOH]+[COO]), and the concentration of polybase, C_B.

For the topological theory of the THL model, the contration of complexed acid groups, [complexed COOH], can be represented as $C_{SC}\ L\ (\Omega/\Omega_{top})$ in consideration of the effect of the topological interaction between polyacids and polybases, whereas in the original theory of Ilopoulos and Audebert, the concentration [complexed COOH] was given by $C_{SC}\ L$ because their theory considered only the contributional terms of complexed points between strands, but not the contributional ones of entangled points and junction points. Then the degree of complexation, θ, is given by

$$\theta=\frac{[\text{complexed COOH}]}{C_A}=\frac{C_{SC}\ L\ (\Omega/\Omega_{top})}{C_A} \tag{18}$$

Therefore,

$$C_{SC}=\frac{\theta\ C_A}{L\ (\Omega/\Omega_{top})} \tag{19}$$

The concentrations C_{SA} and C_{SB} can be given by

$$C_{SA}=C_A\frac{B}{N} \tag{20}$$

and

$$C_{SB}=C_B\frac{B}{N}=\tau\ C_A\frac{B}{N} \tag{21}$$

where τ is represented as the ratio C_B/C_A.

Substituting C_{SC}, C_{SA}, and C_{SB} [Eqs. (19)-(21)] in Eq. (17), we obtain

$$K_{SC}=\frac{L\ (\Omega/\Omega_{top})}{C_A}\cdot\frac{\theta}{[BL(\Omega/\Omega_{top})/N-\theta][\tau BL(\Omega/\Omega_{top})/N-\theta]} \tag{22}$$

If we write K_s of the original Iliopoulos and Audebert's theory so as to compare with Eq. (22), then

$$K_{SC}=\frac{L}{C_A}\cdot\frac{\theta}{[BL/N-\theta][\tau BL/N-\theta]} \tag{22'}$$

Viscosity of Polymer Complexes

Usually the viscosity of a polymer solution depends on the size of macromolecular chains or aggregates. Thus, we must introduce some complementary assumptions about the hydrodynamic volume of the chains and the manner in which, in a given volume of the solution, complexation between acid and base sequences occurs.

In the THL model, each polyacid macromolecule has only a small number, B, of complexable acid sequences and similarly only a few sequences of each polybase macromolecule can be involved in the complexation reaction. Thus, the polymer mixture can be regarded as a polycondensation medium. In such a case, each primary polyacid or polybase macromolecule behave as a multifunctional monomer reacting by its complexable sequences.

The progressive association of the primary chains increases the weight average molecular weight of the macromolecular aggregate—(polycondensate) formed, its hydrodynamic volume and the viscosity of the mixture. Similarly to the case of multifunctional monomers polycondensation, an infinite macroaggregate is formed and gelation occurs associated with a divergence of the viscosity and the weight average molecular weight. It is known that the weight average molecular weight and the gel point can be predicted, depending on the extent of polycondensation reaction (*i.e.*, the degree of complexation), the monomer functionality (the number of distinct polybase chains complexed with one PAA chain) and the stoichiometry.

In polymer complex systems, the interchain condensation reaction may be in competition with intrachain condensation. Thus, the effective functionality, F, of a primary chain (PAA or polybase) will be smaller than the number B of the complexable sequences per chain. Since the polymer mixture is assumed to be very far from bulk state polycondensation, we must take into account the formation of intramolecular reactions which do not correspond to significant expansion of the structure in view of viscosity properties. The role of intramolecular reactions has ever been mentioned in some polycondensation theories.[29] Additionally it is supposed that the medium is homogeneous, *i.e.*, there is no exclusion between complementary macromolecules.

Consider the intramolecular reaction for polymer complexes. An approximate picture of the polycondensation medium is given in Scheme 3. Consider an acid sequence (length L) effectively complexed at a given moment (the vicinal polyacid complexable sequence may be free *i.e.*, not complexed) by the same polybase macromolecule as the first sequence (intramolecular complexation). It is regarded that the balance intramolecular/intermolecular complexation depends on the relative concentration in polybase sequences in the vicinity of the considered polyacid sequences. If the relation between the degree of polymerization and the radius of gyration, R_g, is known, the volume, V, occupied by these PAA sequences (bearing $nL+mM$ monomer units) can be calculated.

Supposing that the polymer solutes behaves as flexible chains in a good solvent, the volume can be given by

$$V=\frac{4}{3}\pi R_g^3 \tag{23}$$

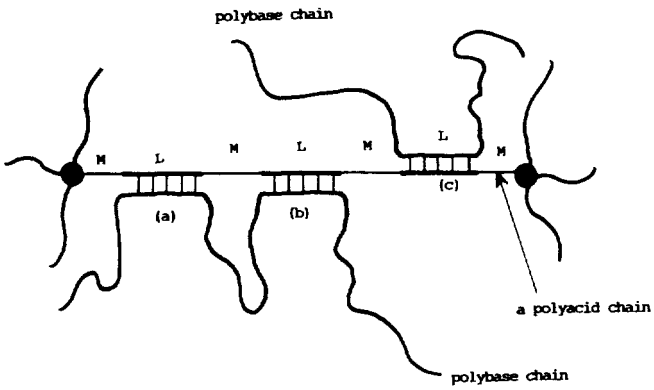

Scheme 3. The complexation between polybase chains and the polyacid chain which is composed of n complexable sequences and m uncomplexable sequences. The relation between part (a) and part (b) is an intrachain complexation, while the relation between part (a) and part (c) is an interchain complexation.

From previous experimental data,[30~33]

$$V=4\times10^{-8}[nL+mM]^{3/5} \text{ (in cm unit)} \tag{24}$$

where n and m are the number of complexable sequences and that of uncomplexable ones, respectively, in the given volume, V. Thus, the volume V is given by

$$V=\frac{4^4}{3}\pi\ 10^{-24}[nL+mM]^{9/5} \text{ (in cm}^3\text{ unit)} \tag{25}$$

Letting the Avogadro's number be N_o, then the average number, N_{SB}, of free complexable polybase sequences per volume unit is given by

$$N_{SB}=\frac{C_A(\tau-\theta)\ N_o}{nL+mM} \tag{26}$$

Referencially speaking, in the original theory of Iliopoulos and Audebert, n and m are all given as two. Actually in order to generalize the topological theory of polymer complexes, in the present work we introduce n and m. Resultantly there are $V\ N_{SB}$ complexable polybase sequences in the volume, V. While the first complexable sequence of the PAA is actually complexed, the remaining number, $N_{SB,V}$ of free complexable polybase sequences in the volume V is given by

$$N_{SB,V}=V\ N_{SB}-1 \tag{27}$$

Then the probability of intrachain reaction in the volume V can be given by

$$A=\frac{1}{N_{SB,V}} \tag{28}$$

Considering Eqs. (25)-(27), we obtain

$$A=\frac{1}{K\ C_A(\tau-\theta)\ (nL+mM)^{4/5}-1} \tag{29}$$

where $K=(4^4/3)\ \pi\ 10^{-27}$ L mol^{-1}.

Consider the extent of reaction for polymer complexes. In general, the extent of complexation reaction, R, can be represented as the probability of a PAA complexable sequence, $R=\theta/\theta_{max}$. The quantity θ_{max} corresponds to the total complexation of the complexable acid sequence ($\theta_{max}=LB/N$).

Now it is the time to consider the functionality of the primary chains. The functionality, F, of the PAA chain is defined as the number of distinct polybase chains complexed with one PAA chain. The quantity F is a function of the probability A, the number B of complexable sequences per PAA chain and the extent of complexation reaction, R.

Based upon the previous procedure of Iliopoulos and Audebert,[13] the vicinal functionality, F_v, is given by

$$F_V=A^{B-1}R^B+(1-RA)\sum_{i=1}^{B-1}A^{i-1}B^i[2+(B-i-1)\ (1-RA)] \tag{30}$$

The quantity F_v has been obtained by considering only the possibility of intrachain reaction between vicinal complexable sequences, which implies F/B, but not the possibility of intrachain reaction between distant sequences. Therefore, the actual functionality, F, describing physical properties of the polymer complexes can be adjusted by introducing the interaction by entanglement between strands in a polymer chain and by considering the interaction caused by the displacement of junction points. Since the functionality F depends on the extent of reaction, F can be briefly derived from Eq. (30) as

$$F_V=A^{B-1}R^B(\Omega/\Omega_{top})^B+[1-R(\Omega/\Omega_{top})A]\sum_{i=1}^{B-1}A^{i-1}B_i(\Omega/\Omega_{top})^i$$
$$[2+(B-i-1)\{1-R(\Omega/\Omega_{top})A\}] \tag{31}$$

Eqs. (22) and (31) are the gist of the present work and the most important equations obtained by our work. In Figure 8, there is plotted the functionality F of a PAA chain against the acrylate ratio. Each PAA macromolecule has a few long complexable sequences (at the limit for $p=0$) when the number of acrylate groups per chain is low ($p\cong0$). When P increases, and it takes a maximum value. Finally it becomes zero for the high acrylate ratios. Alternatively speaking, all the acid sequences become smaller than l_c. Since the number B of complexable sequences per chain increases, the maximum of F increases when l_c decreases.

It is general to use the Durand-Bruneau relation for estimation of the degree of the weight average polymerization of the complex, $(\overline{DP}_w)_{comp}$. That is equal to the average number of acid and base chains per macromolecular aggregate. In the THL model, since all the chains (PAA and primary polybase chains) is assumed to have identical functionalities and the equal degree of polymerization, and to have the contributional terms which are caused by not only complexed points but also physically entangled points and junction points, then the Durand-Bruneau relation is reformed to

$$(\overline{DP}_w)_{comp}=1+\frac{(q_pF)(\Omega/\Omega_{top})[2+q_p(1+1/\tau)[F(\Omega/\Omega_{top})-1]}{1-(1/\tau)\ q_p^2\cdot[F(\Omega/\Omega_{top})-1]^2} \tag{32}$$

where q_p is the ramification probability which is proportional to the extent of complexation. Furthermore, since only F of the B complexable sequences per chain can be transformed to interchain complexation ($F<B$), the quantity q_p is equal to RF/B.

Therefore,

$$(\overline{DP}_w)_{comp} = 1+\frac{(RF^2/B)(\Omega/\Omega_{top})[2+(RF/B)(1+1/\tau)[F(\Omega/\Omega_{top})-1]}{1-(1/\tau)(R^2F^2/B^2)[F(\Omega/\Omega_{top})-1]^2} \quad (33)$$

If we write the original theory of Iliopoulos and Audebert, then

$$(\overline{DP}_w)_{comp} = 1+\frac{(RF_v^2/B)\ [2+(RF_v/B)(1+1/\tau)[F_v-1]}{1-(R^2F_v^2/\tau B^2)\ (F_v-1)^2} \quad (33')$$

It is well known that the degree of weight average polymerization $(\overline{DP}_w)_{comp}$ and the absolute viscosity, η, of a geling system diverge near the gel point.

For the polymer network of the THL model structure, composed of two kinds of polymer solutes in water solvent, the viscosity of the polymer complex system, η, can be represented as follows in view of topological network theories,

$$\eta = \frac{\beta N_o}{DV^2}\left\{\frac{\zeta_A\zeta_B l_{AO}^2 l_{BO}^2}{M_{AO}M_{BO}}\right\}(\overline{DP}_w)_{comp}\alpha[_{[M_A]}\Omega/_{[M_B]}\Omega_{top}-1] \quad (34)$$

In Eq. (34), β is the miscible constant between two kinds of polymer solutes, N_o is the Avogadro's number, D is a diffusion coefficient of the polymer solution, V is the volume of the polymer solution, ζ_A is the friction coefficient of polyA chains, ζ_B is that of polyB chains, l_{AO} is the segmental step length of polyA chains, l_{BO} is the segmental step length of polyB chains, M_{AO} is the molecular weight of the monomer of polyA chains, M_{BO} is that of polyB chains, α is the thermal factor of the aqueous solution, $[M_A]$ is the concentration of the polyA solute, and $[M_B]$ is the concentration of the polyB solute.

Results and Discussion

The results of the Iliopoulos and Audebert's theory for polymer complex systems are expanded by adding those of a topological network theory of dealing with the interaction between strands in order to remove the discrepancy between the original theory of Iliopoulos and Audebert and experimental data nearly to the limit of zero.[13,34~35]

It is supposed that the polymer complex systems considered here are composed of the polymer networks of the THL model. The detailed structure for these polymer networks is plotted in Figure 1. The polymer network of joining the junction points represented by black closed circles is an aggregate of polyacid chains (polyA chains), and that by white open circles is the one of polybase chains (polyB chains).

It is regarded that the THL model offered here is a reasonable polymer network when attractive and repulsive force between chains are all considered. In polymer networks of the THL structure, the way of arranging of strands around junction points is plotted in Figure 2. The essence of topological network theories is based in the fact that the interaction between strands is regarded as the principal contribution term to entropy and free energy for polymer complex systems. Interaction between strands can be classified into the term caused by single contact and that by double. A distance between strands is given by

$$d = \frac{|r_a + r_a' - r_b - r_b'|}{2m^{1/2}a} \quad (35)$$

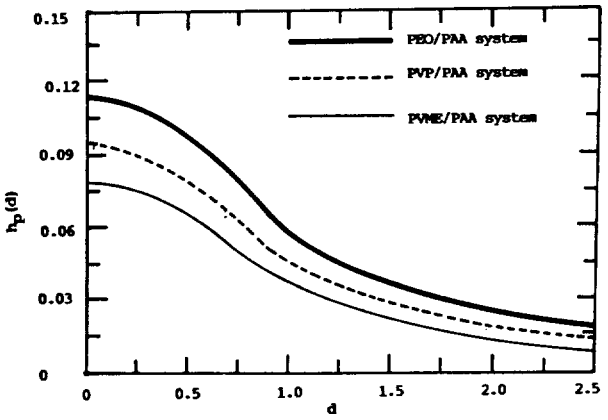

Figure 3. The $h_p(d)$ as functions of d, which is a distance between the centers of the strands, for the THL model. In this picture,there are given the calculated curves for the (a) PEO/PAA, (b) PVP/PAA, and (c) PVME/PAA systems. The thick solid curve (a) represents the one obtained by the PEO/PAA aqueous solution when the root mean squared end-to-end distance of a strand, q, is 0.27 $m^{1/2}a$, the dashed curve (b) represents the one obtained by the PVP/PAA aqueous solution when q is 0.34 $m^{1/2}a$, and the thin solid curve (c) represents that by the PVME/PAA aqueous solution when q is 0.38 $m^{1/2}a$.

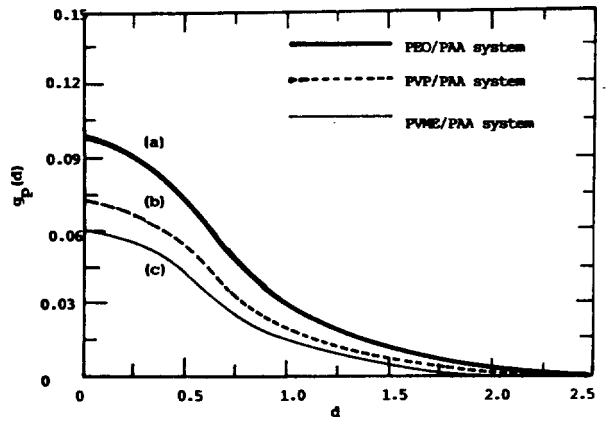

Figure 4. The $g_p(d)$ as functions of d, which is a distance between the centers of the strands, for the THL model. The thick solid curve (a) represents the one obtained by the PEO/PAA aqueous solution when the root mean squared end-to-end distance of a strand, q, is 0.27 $m^{1/2}a$, the dashed curve (b) represents the one obtained by the PVP/PAA aqueous solution when q is 0.34 $m^{1/2}a$, and the thin solid curve (c) represents that by the PVME/PAA aqueous solution when q is 0.38 $m^{1/2}a$.

where r_a and r_a' are the position vectors representing both end points of the a strand, and r_b and r_b' those of the b strand. $g_p(r)$ and $h_p(r)$ of Eq. (3) are shown the calculated curves of $h_p(d)$ about the PEO/PAA, PVP/PAA, and PVME /PAA systems for the THL model structure. In Figure 4, there are shown the calculated curves of $g_p(d)$ about the PEO/PAA, PVP/PAA, and PVME/PAA systems for the THL model structure. In Figures 3 and 4, the thick solid curves (a) represent the ones obtained by the PEO/PAA aqueous solution when the root mean squared end-to- end distance

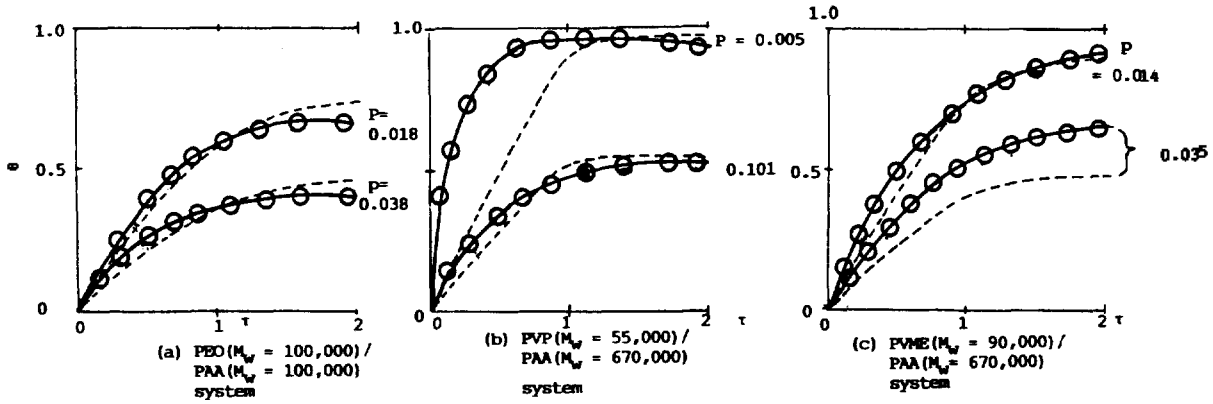

Figure 5. The degree of complexation, q, of three polymer aqueous solution systems, plotted with the given values of acrylate ratio, p, as functions of the relative concentration ratio, τ. The black closed circles of each picture represent the experimental values of each sample.[34] The dashed curves represent the results of the original theory of Iliopoulos and Audebert for the given values of acrylate ratio, p. The solid curves represent the results of our theory for the given values of acrylate ratio, p.

between the centers of strands, q, is 0.27 $m^{1/2}a$, the dashed curves (b) represent the ones obtained by the PVP/PAA aqueous solution when q is 0.34 $m^{1/2}a$, and the thin solid curves (c) represent those by the PVME/PAA aqueous solution when q is 0.38 $m^{1/2}a$. Since the value of q of each sample strand is peculiarly determined by various factors such as degree of polymerization, concentration of solutions, temperature, and so on, the values of q of three sample strands differ respectively. It is selfevident that the farther the distance between strands is, the smaller the probability of contact between strands is. In Figures 3 and 4, the value of $h_p(d)$ is greater than that of $g_p(d)$ since the double contact probability is greater than the single contact one due to the character resulting from the relatively long length of a strand.

In Figure 5, the degree of complexation, θ, of three polymer aqueous solution systems, related to the given values of acrylate ratio, p, is plotted as functions of the relative concentration ratio, τ. The three polymer solution systems are such as (a) PEO/PAA, (b) PVP/PAA, and PVME/PAA systems. The black closed circles of each picture represent the experimental values of each sample.[34] The dashed curves represent the results of the original theory of Iliopoulos and Audebert for the given values of acrylate ratio, p. The solid curves represent the results of our theory for the given values of acrylate ratio, p.

As shown in Figure 5, our theoretical curves are fitted better than those of the original Iliopoulos and Audebert's theory, with data points of each sample. The discrepancy between the data points and the original Iliopoulos and Audebert's theory seems to result from the fact that their theory has considered only the contributional effect of chemically complexed points between strands, but not the contributional effect of junction points and physically entangled points.

In Figure 6, there is shown the influence of the degree of polymerization, N, of PAA on the degree of complexation, u, as functions of the relative concentration ratio, τ. The solid curves represent those of the original theory of Iliopoulos and Audebert for the PEO/PAA system, with $C_A=0.02$ mol·L^{-1} and $p=0.02$. The variation of the degree of

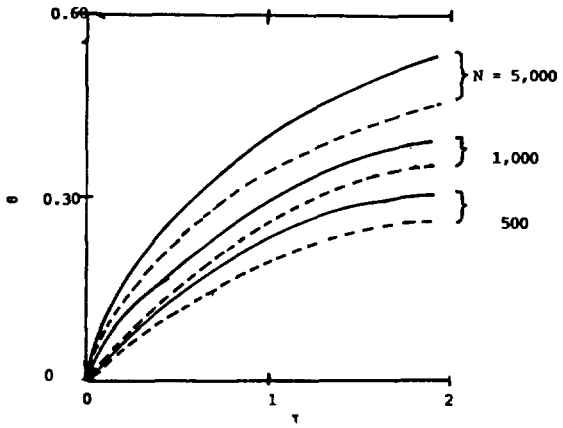

Figure 6. Influence of the degree of polymerization, N, of PAA on the degree of complexation, θ. The solid curves represent those of the original theory of Iliopoulos and Audebert for the PEO/PAA system, with $C_A=0.02$ mol·L^{-1} and $p=0.02$.

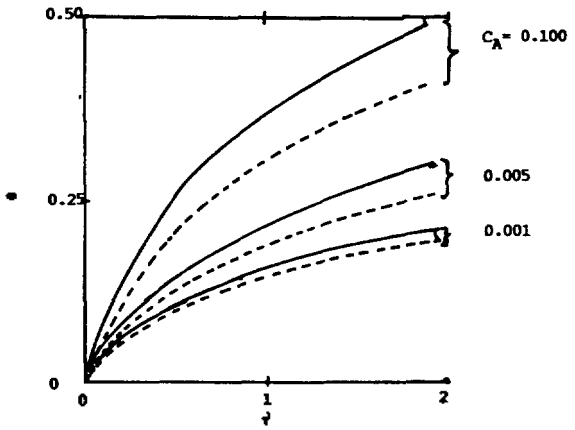

Figure 7. Influence of the polymer concentration, C_A, on the degree of complexation, θ. The solid curves represent the results of our theory, while the dashed curves represent those of the original theory of Iliopoulos and Audebert for the PEO/PAA system, with $N=1{,}000$ and $p=0.04$.

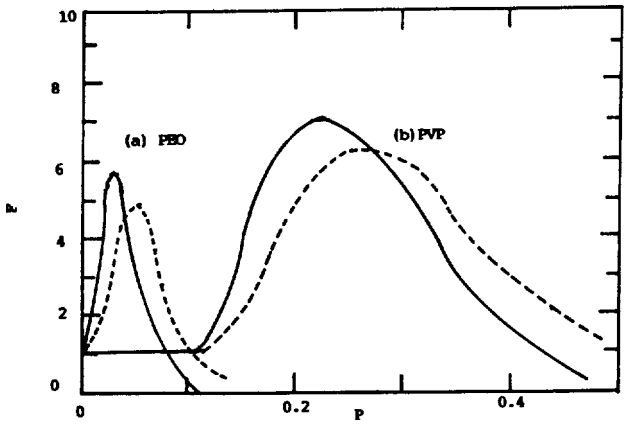

Figure 8. The PAA functionality, F, in the polymer-solvent systems, plotted as functions of the acrylate ratio, p. The theoretical curves near the part (a) are those of the PEO/PAA system, and the curves near the part (b) are those of the PVP/PAA systems, with $N=1{,}000$, $C_A=0.1$ mol·L^{-1}and $\tau=2$. For K_s and l_c, the corresponding values are given in Ref. 13. The solid curves represent the results of our theory, while the dashed curves represent those of the original theory of Iliopoulos and Audebert.

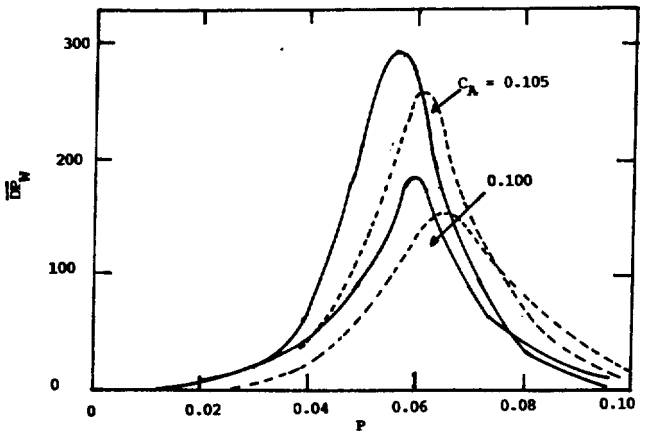

Figure 9. Influence of the polymer concentration, C_A, on $(\overline{DP}_w)_{comp}$. There is shown the weight average degree of polymerization, $(\overline{DP}_w)_{comp}$, , of the polymer complexes, plotted as functions of the inactive concentration ratio, p, for the three given values of the concentration, C_A. The solid curves represent the results of our theory, while the dashed curves represent those of the original theory of Iliopoulos and Audebert for the PEO/PAA system, with $N=1{,}000$ and $\tau=2$.

complexation by the variation amount of the degree of polymerization becomes greater in our topological theory than in the original theory of Iliopoulos and Audebert. It is regarded that in our theory there has been sufficiently considered the effect of interaction by entanglement between strands in polymer chains.

In Figure 7, there is shown the influence of the polymer concentration, C_A, on the degree of complexation, θ. The solid curves represent the results of our theory, while the dashed curves represent those of the original theory of Iliopoulos and Audebert for the PEO/PAA system, with $N=1{,}000$ and $p=0.04$. The variation of the degree of complexation by the

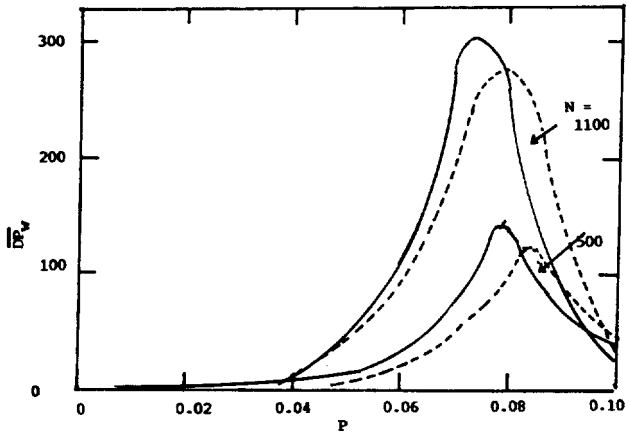

Figure 10. Influence of the degree of polymerization, N, on $(\overline{DP}_w)_{comp}$. There is shown the weight average degree of polymerization, $(\overline{DP}_w)_{comp}$, of the polymer complexes plotted as functions of the inactive concentration ratio (acrylate ratio), p, for the three given values of the degree of polymerization, N. The solid curves represent the results of our theory, while the dashed curves represent those of the original theory of Iliopoulos and Audebertfor the PEO/PAA system, with $C_A=0.05$ and $\tau=2$.

variation amount of the degree of polymerization becomes greater in our topological theory than in the original theory of Iliopoulos and Audebert. Such a tendency seems to arise from the fact in our theory there has been sufficiently considered the effect of interaction by entanglement between strands in polymer chains.

In Figure 8, there is shown the PAA functionality, F, in the polymer-solvent systems, plotted as functions of the acrylate ratio, p. The theoretical curves near the part (a) are those of the PEO/PAA system, and the curves near the part (b) are those of the PVP/PAA systems, with $N=1{,}000$, $C_A=0.1$ mol·L^{-1}, and $t=2$. For K_s and l_c, the corresponding values are given in Ref. 13. The solid curves represent the results of our theory, while the dashed curves represent those of the original theory of Iliopoulos and Audebert. In our theory, the maximum values of functionality of the given polymer solution systems move toward the left side of the axis of the polymer concentration, compared with the original theory of Iliopoulos and audebert.

Such a tendency seems to arise from the fact that the lower the concentration of acrylate groups is, the greater the frequency of contact between strands is.

In Figure 9, there is illustrated the influence of the polymer concentration, C_A, on $(\overline{DP}_w)_{comp}$. There is shown the weight average degree of polymerization, $(\overline{DP}_w)_{comp}$, of the polymer complexes, plotted as functions of the inactive concentration ratio, p, for the three given values of the concentration, C_A. The solid curves represent the results of our theory, while the dashed curves represent those of the original theory of Iliopoulos and Audebert for the PEO/PAA system, with $N=1{,}000$ and $\tau=2$.

In Figure 10, there is illustrated the influence of the degree of polymerization, N, on $(\overline{DP}_w)_{comp}$. There is shown the weight average degree of polymerization, $(\overline{DP}_w)_{comp}$, of the polymer complexes plotted as functions of the inactive concentration ratio (acrylate ratio), p, for the three given values

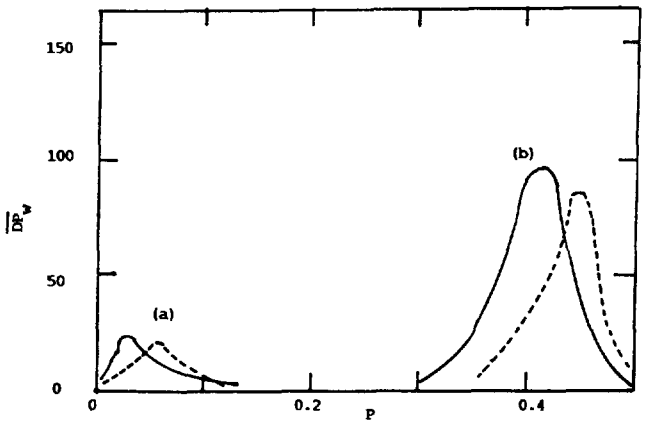

Figure 11. Influence of the critical chain length on $(\overline{DP}_w)_{comp}$. There is shown the weight average degree of polymerization, $(\overline{DP}_w)_{comp}$, of the polymer complexes plotted as functions of the inactive concentration ratio, p, for the PEO/PAA ($l_c=40$) system part (a) and the the PVP/PAA ($l_c=13$) system of part (b), with $N=500$, $\tau=2$, and $C_A=0.075$ mol·L^{-1}. The solid curves represent the results of our theory, while the dashed curves represent those of the original theory of Iliopoulos and Audebert for the polymer systems.

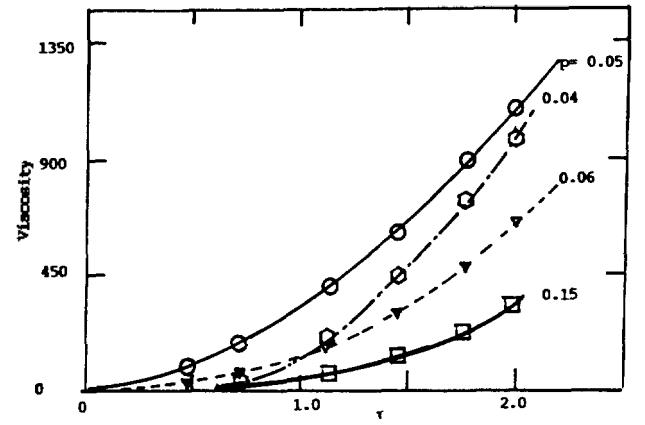

Figure 12. In the PEO/PAA system, the experimental points and theoretical curves for viscosity, plotted as functions of the relative concentration ratio, τ, with the values of the acrylate ratio, p. The experimental data points are represented as diagrams such as squares, triangles, circles, and inverse triangles.

of the degree of polymerization, N. The solid curves represent the results of our theory, while the dashed curves represent those of the original theory of Iliopoulos and Audebert for the PEO/PAA system, with $C_A=0.05$ and $\tau=2$.

In Figure 11, there is illustrated the influence of thecritical chain length on $(\overline{DP}_w)_{comp}$. There is shown the weight average degree of polymerization, $(\overline{DP}_w)_{comp}$, of the polymer complexes plotted as functions of the inactive concentration ratio, p, for the PEO/PAA ($l_c=40$) system of part (a) and the the PVP/PAA ($l_c=13$) system of part (b), with $N=500$, $\tau=2$, and $C_A=0.075$ mol·L^{-1}. The solid curves represent the results of our theory, while the dashed curves represent those of the original theory of Iliopoulos and Audebert for the polymer systems.

Table 1. The values of parameters used in fitting with experimental data.[35]

	ζ_A (10^{-8} kg/s)	ζ_B (10^{-8} kg/s)	α	β	D (10^{-19} m^2/s)
PEO/PAA	12.24	5.26	0.614	0.232	4.23
PVP/PAA	12.43	6.14	0.683	0.318	4.34
PVME/PAA	12.36	6.47	0.715	0.341	4.51

In Figures 9-11, the results (*i.e.*, the values of curves) obtained by our theory shift to the side lefter than in those of the original Iliopoulos and Audebert's theory. Such a tendency seems to arise from the fact that in the original theory of Iliopoulos and Audebert there has been considered only the effect caused by the displacement of chemically complexed points in strands, whereas in our theory there has been sufficiently considered the effect caused not only by complexed points but also by entangled points and junction points.

In Figure 12, for the PEO/PAA system, there are shown the experimental points and theoretical curves for viscosity, plotted as functions of the relative concentration ratio, τ, with the values of the acrylate ratio, p. The experimental data points are represented as diagrams such as squares, triangles, circles, and inverse triangles. It is shown that the theoretical curves are well fitted with experimental data.[35]

In Table 1, there given the values of parameters used in fitting with experimental data.[35] The physical meanings of these parameters are self-evident as shown previously.

Conclusion

The original theory of Iliopoulos and Audebert about polymer complex aqueous solution systems has been extended by considering topologically the contributional terms caused by the displacement of physically entangled points and junction points. Thus our extended theory explains very well the characteristics of the degree of complexation and the viscosity of polymer complex systems. The polymer complex systems considered here are supposed to have the structure of the THL network composed of polymer solutes and solvent. It is judged that the discrepancy between the experimental data and the original Iliopoulos and Audebert's theory results from the fact that their original theory did not include the results of interaction caused by entangled points and junction points.

It is exposed that the results of the extended theory show good agreement with the given experimental data.

Finally, it is judged that assumption of the THL structure for the given polymer complex systems is very reasonable, based upon the fact that the extended theory explains very well the given experimental data.

Acknowledgment. The Present Studies were Supported (in part) by the Basic Science Research Institute Program, Ministry of Education, 1995. Project No. BSRI-95-3414.

References

1. Flory, P. J.; Rehner, J. J. *J. Chem. Phys.* **1943**, *11*, 521.
2. Edwards, S. F.; Freed, K. F. *J. Phys. C.* **1970**, *3*, 760.

3. Graessley, W. W. *Macromolecules* **1975**, *8*, 865.
4. Ronca, G.; Allegera, G. *J. Chem. Phys.* **1975**, *63*, 4990.
5. Flory, P. J. *Proc. R. Soc. London Ser. A.* **1976**, *351*, 351.
6. Ziabicki, A.; Walasek, J. *Macromolecules* **1978**, *11*, 471.
7. Langley, N. R. *Macromolecules* **1968**, *1*, 348.
8. Deam, R. T.; Edwards, S. F. *Philos. Trans. R. Soc. London Ser. A* **1976**, *280*, 317.
9. Graessley, W. W.; Pearson, D. S. *J. Chem. Phys.* **1977**, *66*, 3363.
10. Iwata, K.; Kurata, M. *J. Chem. Phys.* **1969**, *50*, 4008.
11. Iwata, K. *J. Chem. Phys.* **1980**, *73*, 562: **1981**, *74*, 2039: **1983**, *78*, 2778: **1985**, *83*, 1969.
12. Iwata, K. *J. Chem. Phys.* **1982**, *76*, 6363: **1982**, *ibid* 6375.
13. Iliopoulos, I.; Audebert, R. *J. Polymer Sci.* **1988**, *26*, 2093.
14. Son, J. M.; Pak, H. *Bull. Korean Chem. Soc.* **1989**, *10*, 84.
15. Son, J. M.; Pak, H. *Proc. Coll. Natur. Sci., SNU* **1988**, *13*, 47.
16. Son, J. M. *Ph. D. Thesis, SNU, Seoul, Korea,* 1989.
17. Son, J. M.; Pak, H. *Bull. Korean Chem. Soc.* **1995**, *16*, 169.
18. Son, J. M.; Pak, H. *Bull. Korean Chem. Soc.* **1995**, *16*, 269.
19. Flory, P. J. *J. Chem. Phys.* **1942**, *10*, 51.
20. Bekturov, E. A.; Bimendina, L. A. *Adv. Polym. Sci.* **1981**, *41*, 99.
21. Tsuchida, E.; Abe, K. *Adv. Polym. Sci.* **1982**, *45*, 2.
22. Zezin, A. B.; Kabanov, V. A. *Russ. Chem. Rev.* **1982**, *51*, 833.
23. Kabanov, V. A.; Papisov, I. M. *Vysokomol. Soyed.* **1979**, *A21*, 243.
24. Baranovsky, V. Y.; Litmanovich, A. A.; Papisov, I. M.; Kabanov, V. A. *Eur. Polym. J.* **1981**, *17*, 969.
25. Anufrieva, E. V.; Pautov, V. D.; Papisov, I. M.; Kabanov, V. A. *Dokl. Akad. Nauk SSSR* **1977**, *232*, 1096.
26. Tsuchida, E.; Osada, Y.; Ohno, H. *J. Macromol. Sci. Phys.* **1980**, *B17*, 683.
27. Osada, Y. *J. polym. Sci. Polym. Chem. Ed.* **1979**, *17*, 3485.
28. Ikawa, T.; Abe, K.; Honda, K.; Tsuchida, E. *J. Polym. Sci. Polym. Chem. Ed.* **1975**, *13*, 1505.
29. Stanford, J. L.; Stepto, R. F. T. *Br. Polym. J.* **1977**, *9*, 124.
30. Mabire, F.; Audebert, R.; Quivoron, C. *Polymer* **1984**, *25*, 1317.
31. Kulicke, W. M.; Kniewske, R.; Klein, J. *Prog. Polym. Sci.* **1982**, *8*, 373.
32. Francois, J.; Sarazin, D.; Schwartz, T.; Weill, G. *Polymer* **1979**, *20*, 969.
33. Allen, G.; Booth, C.; Hurst, S. J.; Jones, M. N.; Price, C. *Polymer* **1967**, *8*, 391.
34. Iliopoulos, I.; Audebert, R. *Eur. Polym. J.* **1988**, *24*, 171.
35. Iliopoulos, I.; Halary, J. L.; Audebert, R. *J. Polym. Sci. Polym. Chem. Ed.* **1988**, *26*, 275.

Photopolymerization of Methyl Methacrylate with Primary Aryl- and Alkylsilanes

Hee-Gweon Woo*, Lan-Young Hong, Soo-Yeon Yang, Sun-Hee Park, Sun-Jung Song, and Heui-Suk Ham

Department of Chemistry, Chonnam National University, Kwangju 500-757, Korea

Received July 8, 1995

The bulk photopolymerization of methyl methacrylate (MMA) with primary arylsilane (e.g., phenylsilane) and various primary alkylsilanes (e.g., benzylsilane, 3-phenoxyphenyl-1-silabutane, 3-naphthyl-1-silabutane, and 3-chlorophenyl-1-silabutane) was performed to produce poly(MMA)s containing the corresponding silyl moiety as an end group. It was found for the phenylsilane that while the polymerization yields increased and then decreased with a turning point at the molar ratio of MMA : silane = 10 : 1 as the relative silane concentration increases, the polymer molecular weights decreased, and the TGA residue yields and the relative intensities of SiH IR stretching bands increased with increment of molar ratio of silane over MMA. The photopolymerization yield of MMA with the arylsilane was found to be higher than those with the alkylsilanes and without the silanes. Thus, the silanes seemed to significantly influence on the photopolymerization as both chain initiation and chain transfer agents.

Introduction

A great amount of attention has been paid to photopolymerization of vinyl monomers because of its distinct advantages such as convenience and the avoidance of chemical contamination by initiator residues. Photopolymerization technology is employed on a commercial scale today in the areas of surface coatings, photoresists, adhesives, and holography.[1] Any vinyl monomer that will undergo chain reaction polymerization is subject to photopolymerization or photosensitized polymerization, but only a few unsaturated monomers are known to absorb light between 250 and 500 nm which is the most convenient wavelength range for experimental work. Methyl methacrylate is susceptible to direct